Biomaterials 31 (2010) 7631–7639

Contents lists available at ScienceDirect

Biomaterials

journal homepage: www.elsevier.com/locate/biomaterials

Intrathecal delivery of a polymeric nanocomposite hydrogel after spinal cord injury

M. Douglas Baumann [a,b,c], Catherine E. Kang [a,b,c], Charles H. Tator [d], Molly S. Shoichet [a,b,c,e,f,*]

[a] Department of Chemical Engineering and Applied Chemistry, University of Toronto, 200 College Street, Toronto, Ontario M5S 3E5, Canada
[b] Institute of Biomaterials and Biomedical Engineering, 164 College Street, Toronto, Ontario M5S 3G9, Canada
[c] Terrence Donnelly Centre for Cellular and Biomolecular Research, 160 College Street, Toronto, Ontario M5S 3E1, Canada
[d] Krembil Neuroscience Centre, Toronto Western Research Institute, and Department of Surgery, University of Toronto, 399 Bathurst Street, Toronto, Ontario M5T 2S8, Canada
[e] Institute of Medical Science, University of Toronto, 1 King's College Circle, Toronto, Ontario M5S 1A8, Canada
[f] Department of Chemistry, University of Toronto, 80 St. George Street, Toronto, Ontario M5S 3H6, Canada

ARTICLE INFO

Article history:
Received 4 June 2010
Accepted 1 July 2010
Available online 24 July 2010

Keywords:
Spinal cord injury
Drug delivery
Hydrogel
Nanoparticles
Hyaluronan
Methylcellulose

ABSTRACT

Major traumatic spinal cord injury (SCI) results in permanent paralysis below the site of injury. The effectiveness of systemically delivered pharmacological therapies against SCI can be limited by the blood–spinal cord barrier and side effects. Local drug delivery to the injured spinal cord can be achieved using a minimally invasive biopolymer matrix of hyaluronan and methylcellulose injected into the intrathecal space, bypassing the blood–spinal cord barrier and overcoming limitations of existing strategies. Composite hydrogels of drug-loaded poly(lactide-*co*-glycolide) (PLGA) nanoparticles dispersed in this biopolymer matrix meet the *in vitro* design criteria for prolonged local release. Using a blank (without drug) composite designed for 28-day sustained release, we presently explore the mechanism of particle-mediated hydrogel stabilization *in vitro* and aspects of biocompatibility and safety *in vivo*. The composite hydrogel is well tolerated in the intrathecal space of spinal cord injured rats, showing no increase in inflammation, scarring, or cavity volume relative to controls, and no significant effect on locomotor function up to 28 days. Furthermore, there was no effect on locomotor function in healthy animals which received the composite hydrogel, although a qualitative increase in ED-1 staining was apparent. These data support the further development of composite hydrogels of hyaluronan and methylcellulose containing PLGA nanoparticles for sustained local delivery to the injured spinal cord, an application for which there are no approved alternatives.

1. Introduction

Traumatic spinal cord injury (SCI) is a devastating condition which results in life-long disability for the majority of patients. Acute injury is estimated at 10,000 cases per year in the United States, and those living with SCI number in the hundreds of thousands [1]. Although there is no cure for SCI, advances in molecular medicine based on improved understanding of the pathophysiology of injury have yielded promising results in animal models [2–4]. These molecules are aimed at either protecting surviving tissue from degeneration or restoring function already lost. Neuroprotective therapies are often delivered in the hours to days after injury, coinciding with the peak of the inflammatory response and other secondary mechanisms of injury [5,6]. In contrast, neuroregenerative therapies are often delivered for several days to weeks, corresponding to the timeframe required to promote repair [7,8]. Delivery of both neuroprotective and neuroregenerative factors is complicated by the blood–spinal cord barrier (BSCB) and the physical inaccessibility of the cord. Since most therapeutic molecules do not cross the BSCB, oral and intravenous delivery cannot be used, leaving the alternatives of local epidural or intrathecal delivery by either bolus injection or indwelling catheter/minipump [3,4,9]. Other methods include direct injection into the spinal cord of, for example, genetically engineered cell grafts [2,10,11], stem cells [12,13], or intraspinal drug eluting implants [14–16]. While promising in animal models, these strategies have risks of immunogenicity, infection, and damage to the cord which often preclude their being tested clinically. At present there is no effective treatment to restore function after major SCI in humans [17].

An ideal drug delivery platform must achieve localized and sustained release and a favourable risk/benefit ratio in order to be

* Corresponding author. Terrence Donnelly Centre for Cellular and Biomolecular Research, 514-160 College Street, Toronto, Ontario M5S 3E1, Canada. Tel.: +1 416 978 1460; fax: +1 416 978 4317.
E-mail address: molly.shoichet@utoronto.ca (M.S. Shoichet).

0142-9612/$ – see front matter © 2010 Elsevier Ltd. All rights reserved.
doi:10.1016/j.biomaterials.2010.07.004

adopted clinically. Developing a safe delivery strategy is therefore an important step in preparing a drug candidate for clinical evaluation. A delivery strategy that allows sustained delivery of multiple molecules at different rates is also desirable given that it is unlikely that a single therapeutic agent will overcome SCI [18]. To this end, we have pursued the design of an intrathecal drug delivery system capable of releasing one or more drugs directly into the spinal cord for up to 28 days. The ideal system would provide local and sustained release (to maximize benefit), be injected in a single dose in a minimally-invasive manner, be biodegradable and non-inflammatory in the CNS (to minimize risk). Previous reports have demonstrated that hydrogels remain localized at the site of injection, are safe [19–21], and provide short term delivery of neuroprotective molecules [22,23]. The surgical protocol for injecting drug-loaded hydrogels into the intrathecal space has been validated in the clip compression model of SCI [19,20,22,23], which closely resembles the most frequent type of clinical SCI [24]. Moreover the intrathecal injection is minimally invasive, especially when combined with surgical decompression, which is an established practice option in North America [25].

In the current study we evaluated the effect of a nanoparticle loaded hydrogel on uninjured rats and rats with clip compression SCI. Our study used a blank (drug free) formulation designed for 28-day drug delivery based on design criteria including: fast gelation, minimal *in vitro* swelling, slow degradation, and sustained drug release [26]. The Basso–Beattie–Bresnahan (BBB) scale of locomotor function was used as an outcome measure to assess safety while cavity volume was used as a gross measure of injury severity. Macrophage activity was quantified to determine if the inflammatory response induced when PLGA is implanted in CNS parenchyma [27–29] would also occur when the PLGA containing composite was injected in the intrathecal space, where it is separated from the parenchyma by the pia mater. Lastly, the effect of the composite hydrogel on astrocyte reactivity was investigated because astrogliosis may inhibit regeneration [30].

The composite is a physical hydrogel of the polysaccharides hyaluronan (HA) and methylcellulose (MC) with dispersed poly (lactide-*co*-glycolide) (PLGA) nanoparticles. MC is inverse thermal gelling, being a viscous fluid at room temperature and a gel at 40–50 °C [31]. Gelation is entropically driven by the release of ordered water from methyl rich regions of the polymer and the resulting association of these hydrophobic domains. The gelation temperature can be reduced below 37 °C by addition of ions, including buffer salts [32] and organic polyelectrolytes, which compete for solvent molecules in a process known as salting out. HA is an anionic polysaccharide of D-glucuronic acid and N-acetyl-D-glucosamine which is shear thinning and salts out MC to form injectable, fast gelling and thermally reversible hydrogels below 37 °C [19]. Fast gelation is critical to ensure the hydrogel remains localized in the fluid-filled intrathecal space after injection. PLGA nanoparticles were dispersed in the hyaluronan and methylcellulose hydrogel (HAMC) as a means to enable sustained drug release and were found to stabilize the hydrogel. Thus, the composite HAMC used here differs from previous HAMC formulations in the composition and molar mass of HA and MC and inclusion of 10 wt% biodegradable nanoparticles [19,23]. These polymers were selected because of their known biocompatibility in the CNS. MC has been used to fill lesions in the brain [33], intrathecally as a gel [19,23,34] and as a sheet [35]. Hyaluronan was selected because it is native to the CNS where it can be anti-inflammatory [19,36], and previous work has demonstrated its biocompatibility specifically when in contact with the meninges [36,37]. HAMC itself has been shown to be well tolerated but it is not known if the PLGA particle loaded composite hydrogel will induce any deleterious tissue responses. PLGA and its degradation products are often found to have acceptable tissue responses, yet they can also be inflammatory [38–41]. This HAMC/PLGA composite system was tested for its safe use in the injured spinal cord, with a view to its use as an intrathecal delivery system for sustained drug release.

2. Materials and methods

2.1. Materials

The following materials were used: sodium hyaluronate of 2600 kg/mol (Lifecore, Chaska, USA); methylcellulose of 300 kg/mol (Shin-Etsu, Tokyo, Japan); poly(D,L-lactic-*co*-glycolic acid) 50:50 of inherent viscosity 0.15–0.25 dL/g (Sigma–Aldrich, Oakville, Canada); poly(vinyl alcohol), 6 kg/mol and 80 mol% hydrolyzed (Polysciences Inc., Warrington, USA); and HPLC grade dichloromethane (DCM) (Caledon Labs, Georgetown, Canada).

The following agents were obtained for the immunohistochemical studies: mouse anti-glial fibrillary acidic protein (GFAP) monoclonal antibody (Millipore, Billerica, USA); mouse anti-rat ED-1 monoclonal antibody (AbD Serotec, Kidlington, UK); and the fluorescent secondary antibody, anti-mouse IgG Alexa Fluor 488 (Invitrogen, Carlsbad, USA). ED-1 is an anti-CD68 IgG.

All buffers were prepared with distilled and deionized water from a Millipore Milli-RO 10 Plus and Milli-Q UF Plus at 18MΩ resistance (Millipore, Bedford, USA). Phosphate buffered saline powder was purchased from MP Biomedicals (pH 7.4, 9.55 g/L, Solon, USA). Artificial cerebrospinal fluid (aCSF) was prepared at a pH of 7.4 and contained: 148 mM NaCl, 3 mM KCl, 0.8 mM $MgCl_2$, 1.4 mM $CaCl_2$, 1.5 mM Na_2HPO_4, and 0.2 mM NaH_2PO_4. All other solvents and reagents were supplied by Sigma–Aldrich and used as-received.

2.2. Preparation of HAMC hydrogels

Physical hydrogel blends of HA and MC were prepared in aCSF at 1 wt% 2600 kg/mol HA and 3 wt% 300 kg/mol MC as previously reported (1:3 HMW HAMC [26]). Briefly, sterile MC and HA were sequentially mechanically dispersed in aCSF and allowed to dissolve at 4 °C. To form composite 1:3 HMW HAMC a slurry of PLGA nanoparticles in aCSF was added to an HMW HAMC solution to produce a nanocomposite hydrogel of 1 wt% HA, 3 wt% MC, and 10 wt% PLGA. The nomenclature is hereafter abridged to HAMC for gels alone and to composite HAMC for nanoparticle loaded gels.

2.3. Preparation of PLGA nanoparticles

PLGA nanoparticles were prepared from a water–oil–water double emulsion as previously described [26]. PLGA nanoparticles were isolated, washed, lyophilized, and stored at −20 °C. Particle size was determined by dynamic light scattering to be 252 nm with a polydispersity of 0.112 (Zetasizer Nano ZS; Malvern Instruments, Malvern, UK).

2.4. Rheological characterization of HAMC hydrogels

The storage moduli of HAMC, HA, and MC with and without nanoparticles were determined as a function of time on a controlled stress rheometer fitted with a 60 mm, 1° acrylic cone and plate geometry (AR-1000; TA Instruments, New Castle, USA). An amplitude sweep was performed to confirm that the frequency and strain were within the linear viscoelastic region. Based on these results, time sweeps were conducted at 6.28 rad/s and 1% strain for all materials. Temperature was controlled using the integrated Peltier plate and sample evaporation was minimized using a solvent trap and supplementary ambient humidification. All samples were equilibrated for 10 min at 4 °C prior to testing at 37 °C. Reversible gelation experiments consisted of three cycles each of 300 min at 37 °C followed by 20 min at 4 °C.

2.5. Intrathecal delivery of composite HAMC in vivo

All animal procedures were performed in accordance with the Guide to the Care and Use of Experimental Animals (Canadian Council on Animal Care) and protocols were approved by the Animal Care Committee of the Research Institute of the University Health Network.

Eight female Sprague Dawley rats (250–300 g; Charles River, Montreal, Canada) were used to assess the effect of HAMC injected into the intrathecal space of uninjured animals on behaviour and immunohistochemistry. Two groups were compared, uninjured and injured rats. In the uninjured group, 4 animals were injected with 10 μL of HAMC and 4 animals were injected with 10 μL of composite HAMC. Injections of aCSF were not included in this study because the safety of intrathecal injection has been previously established [19,20]. Uninjured rats were anaesthetized by inhalation of 1–2% halothane and a laminectomy was performed at the T1-T2 vertebral level. The intrathecal injection was performed with minor modification of the methods initially described by Jimenez-Hamann et al. [20]. Briefly, the dura was punctured with a bevelled 30G needle at T2, a 30G blunt-tipped needle was inserted into the intrathecal space, and 10 μL of sterile HAMC or

composite HAMC pre-heated to 37 °C was injected. Following injection the overlying muscles and fascia were sutured closed and the rats were ventilated with pure oxygen and placed under a heat lamp for recovery. Buprenorphine was administered every 12 h for 3 days post-surgery for pain management. Motor function was assessed weekly as-described below. The animals were sacrificed 14 days after surgery and perfused intracardially with 4% paraformaldehyde under terminal anaesthesia with sodium pentobarbital. A 20 mm segment of spinal cord encompassing the injury site was harvested from each animal, dehydrated in 30% sucrose, and stored at −80 °C until cryoprocessing.

In the second group, 30 female Sprague Dawley rats (250–300 g; Charles River) were used to assess the behavioural and tissue responses of HAMC injected into the intrathecal space of injured animals relative to aCSF. Surgical procedures were identical to those described above except that, prior to injection of HAMC or composite HAMC, all animals sustained moderate clip compression SCI at T2 using a modified aneurysm clip calibrated to a closing force of 26 g for 60 s, as previously described [42]. Animals were then allocated to one of three subgroups ($n = 10$ per subgroup): 10 μL injection of aCSF (control), 10 μL of HAMC, or 10 μL of composite HAMC. Post-surgical animal care was likewise similar, with the addition of manual rat bladder expression three times daily. Motor function was assessed weekly and the animals sacrificed 28 days after surgery. Spinal cords were processed for histological and immunohistochemical analyses as-described below.

2.6. Histology and immunohistochemistry

For injured rats, four cords per subgroup were sectioned parasagittally at 20 μm thickness on a cryostat (CM 3050 S; Leica Microsystems, Wetzlar, Germany). Every 10th section in the clip compression rats was stained with Luxol Fast Blue, and counter-stained with hematoxylin and eosin (LFB/H&E). Images were captured by bright-field microscopy (Scanscope XT; Aperio Technologies, Vista, USA) at 20× objective magnification, examined for general tissue morphology, and cavity area quantified with an image analysis system for all sections (Image J; Wayne Rasband, Bethesda, USA). Cavity volume was calculated by multiplying the area per section by distance between sections.

Fluorescent microscopy was used to assess ED-1 staining at 10× objective magnification (BX-61; Olympus, Tokyo, Japan). The full 20 mm length of spinal cords in 6 sections was imaged in both uninjured and injured rats and the resulting image sets were tiled in Adobe Photoshop (Createive Suite 3, San Jose, USA). The area of ED-1 staining was then quantified for the clip compression study using Image J. The sections were taken at ±50, 150, and 250 μm on each side relative to the midline of the cord. The result is reported as the percentage of ED-1 labelled tissue relative to total tissue area in a given parasagittal section. GFAP staining in the clip compression study was determined and reported in a similar manner. Preliminary analysis of the 20 mm sections found measurable staining only in the rostro-caudal region surrounding the cavity. An area of interest extending ±1.25 mm from the cavity epicentre was therefore selected to more precisely quantify GFAP stained tissue. The area of GFAP staining was quantified in two sections per animal at ±50 μm relative to the midline: it was not possible to determine the number of GFAP positive cells in the area of interest due to the high density of staining.

2.7. Functional analysis

Open field locomotor function was assessed using the Basso, Beattie, and Bresnahan (BBB) scoring method [43] weekly for either two weeks (uninjured animals) or four weeks (injured animals). Each hind limb was ranked by two blinded observers and concurrently videotaped. BBB scores range from 0 (no hind limb movement) to 21 (normal gait) and are used to assess functional improvement after injury and treatment. BBB was performed in uninjured animals to determine if the materials had any early detriment to normal motor function.

2.8. Statistical analysis

Data are expressed as means ± standard deviation. Comparisons of groups of means were determined by ANOVA. Significance was assigned at $p < 0.01$.

3. Results

3.1. Rheology

The storage modulus, G′ was compared between MC and HAMC, with and without nanoparticles to gain a greater understanding of the impact of HA and nanoparticles on the rheological behaviour of the composite. As shown in Fig. 1a, MC alone stiffens over time at 37 °C, an effect attributed to the optimization of hydrophobic junctions [44]. Addition of HA immediately results in a 6-fold increase in G′ over MC alone. The increased storage modulus is attributed to HA salting out MC, thereby enhancing the hydrophobic interactions between MC methyl groups [32]. Unexpectedly, the addition of PLGA nanoparticles to both MC and HAMC also increased G′, up to 7-fold for composite MC and over 2-fold for composite HAMC. The fold increase in G′ increased substantially over time for composite hydrogels, thereby differentiating the effect of nanoparticles on G′ from that of HA. To determine whether nanoparticle-induced stiffening was reversible, the elastic modulus of MC and composite MC were measured as functions of time over three temperature cycles between 4 °C and 37 °C, shown in Fig. 1b. In each case the samples returned to the initial G′ (4 °C), confirming the reversible inverse thermal gelation of composite MC. The altered rheology of composite MC and HAMC is likely due to hydrophobic interactions between MC di- and tri-methylglucose units and hydrophobic PLGA nanoparticles similar to that observed in other composite hydrogels [45].

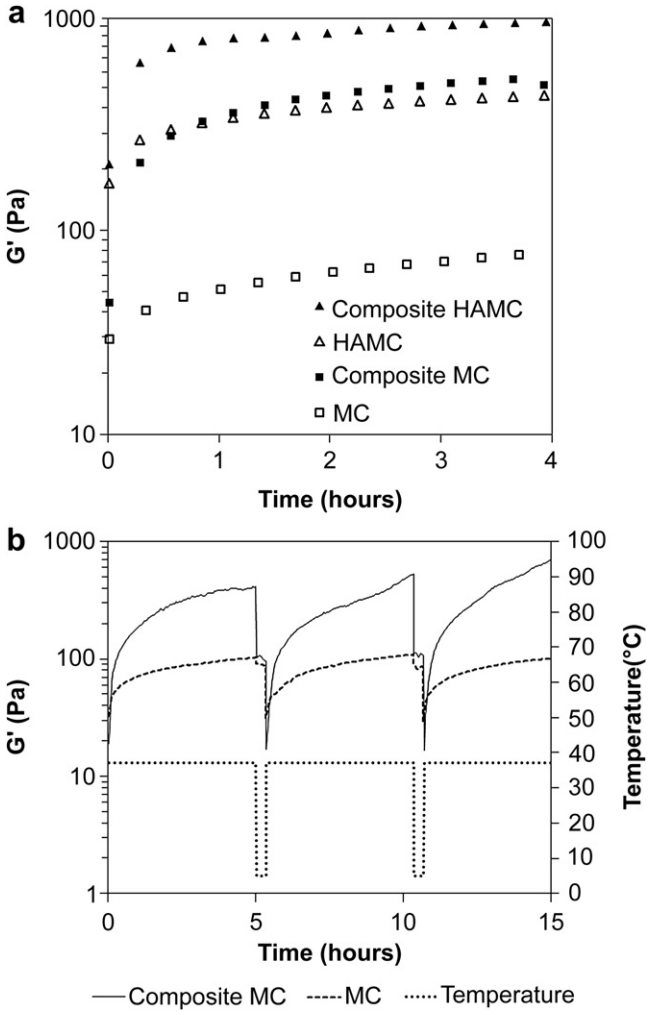

Fig. 1. HA and nanoparticles dramatically stiffen MC, but through different mechanisms. In a), the intrinsic salting out of MC by HA is immediately evident in a 6-fold increase in initial G′. The effect of nanoparticles on MC is of similar magnitude, and likely due to a hydrophobic association similar to the MC–MC interactions responsible for the inverse thermal gelation of MC. The reversible gelation of MC and composite MC is shown in b), where the presence of nanoparticles enhances G′(t, T) at 37 °C but not 4 °C.

3.2. Motor function and tissue response in uninjured rats

Animals in the uninjured cohort underwent laminectomy and intrathecal injection on day 0 and were sacrificed on day 14. The

dorsal half of the spinal cord which had been in direct contact with the composite was stained with ED-1 for activated macrophages. Parasagittal sections taken at the midline of each cord were examined for a distance of ±10 mm from the site of injection. Animals which received HAMC had negligible ED-1 staining, as shown in Fig. 2a, indicating that the hydrogel alone does not induce an inflammatory response. This result is in agreement with our earlier work with a different formulation of HA and MC [19]. Animals that received composite HAMC displayed discrete, scattered staining in regions in contact with the composite, ±5 mm from the injection site, at a thickness of up to 40 μm (1–2 cell diameters).

Function was assessed using the 21-point BBB scoring system [43] at 0, 7, and 14 days as-reported in Fig. 2c. All of the HAMC and composite HAMC injected animals had a BBB score of 21 at each time point, indicating that neither HAMC nor composite HAMC negatively affected motor function in uninjured rats. These important results led us to evaluate these materials in an injured paradigm.

3.3. Motor function and tissue response in spinal cord injured rats

Animals in the clip compressed cohort underwent laminectomy, clip compression spinal cord injury and intrathecal injection on day 0 and were sacrificed on day 28. Parasagittal sections were stained with LFB/H&E to assess cavity shape and volume. The cavity was spindle-shaped in all animals, most often with a thin rim of spared tissue at the injury epicentre as shown in Fig. 3a, which is typical of a compression injury [46]. No variation in cavity shape was found between HAMC, composite HAMC, and aCSF control groups. The mean cavity volume was 3.89 ± 0.87 mm^3 for HAMC-treated animals and 4.57 ± 2.10 mm^3 for composite HAMC-treated animals. These values were not significantly different from the volume of 3.96 ± 1.09 mm^3 for the aCSF control reported in Fig. 3b and indicate neither HAMC nor composite HAMC increased cavitation relative to the aCSF control.

A second series of parasagittal sections was stained with ED-1 for activated macrophages and the section examined ±10 mm from the site of injury. Prominent and continuous staining was found surrounding the cystic cavity, often extending rostro-caudal along the midline of the cord. Scattered macrophage activation was present throughout the cord, as shown in Fig. 4a, often along the full 20 mm length of interest. No variation in the pattern of inflammation was noted between groups. There were no significant differences in the area of inflammation between groups, shown in Fig. 4b.

GFAP staining for astrogliosis after injury was concentrated in the rim of remaining tissue and in long continuous stretches bordering the cystic cavity, shown in Fig. 5a. The area of interest encompassed both the most heavily degenerated tissue within the cord and the surface of the cord in contact with the hydrogel. Discrete GFAP staining was also seen in the tissue immediately surrounding the injury. Analysis of the area of GFAP staining (Fig. 5b) showed no significant differences in astrogliosis between groups, indicating that neither HAMC nor the composite increased the area of tissue occupied by reactive astrocytes following injury.

Function was assessed using the BBB locomotor scoring system weekly up to 28 days, as-reported in Fig. 6. All animals showed nominal improvement over 28 days, as is typical for this severity of injury with this model [42]. Control animals with an aCSF injection reached a maximum plateau score of 11.6 ± 0.8; HAMC injected animals, 11.0 ± 0.5; and composite HAMC injected animals, 11.0 ± 0.5. There were no statistically significant differences between groups within each time point, indicating that neither HAMC nor composite HAMC negatively affected motor function in clip compression SCI rats.

4. Discussion

HA is a polyelectrolyte and should therefore enhance the formation of hydrophobic interactions between MC through the salting out effect [32], resulting in a lower temperature of gelation than would normally be possible with MC alone. This effect is an intrinsic property of the anionic HA and affects MC across a range of molecular weights and temperatures. Indeed, the HA induced stiffening of MC is present even when HA molecular weight is reduced to 35 kg/mol (data not shown), significantly below the accepted entanglement threshold for physical cross-linking [47]. This confirms that HA and inorganic ions work to salt out MC by the same mechanism. Yet unlike simple salts HA forms a viscous, shear thinning solution, providing the HAMC blend with fast gelation at physiological temperature while still allowing the HAMC blend to flow through a fine 30-gauge needle. An ancillary effect of HA is the osmolarity driven increase in the HAMC swelling ratio [26]. To ensure that polyelectrolyte induced swelling of the hydrogel would not induce a deleterious tissue response *via* compression of the cord or obstruction of CSF flow [48,49], the hydrogel and composite

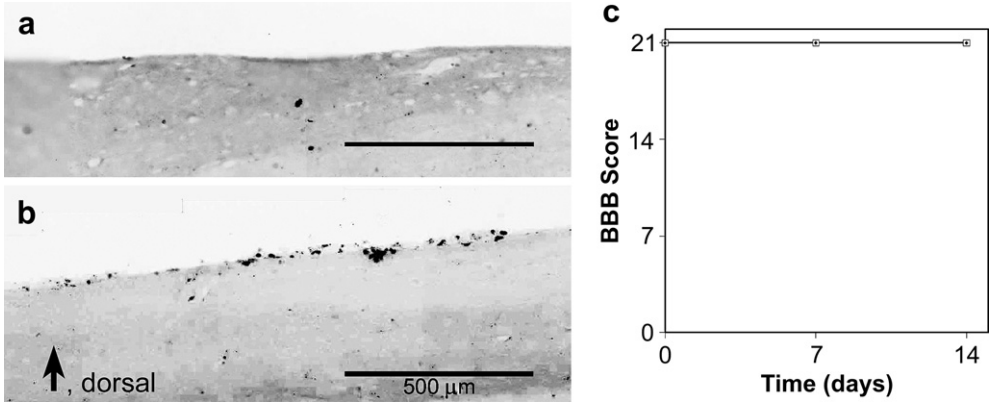

Fig. 2. The inflammatory response marked by ED-1 positive macrophages is a) negligible 14 days after HAMC injection and b) mild to moderate after composite HAMC injection. Images are contrast enhanced to show ED-1 staining (dark specks) and surrounding tissue (gray). Images are representative sections taken from the dorsal aspect of parasagittal sections centred at the site of injection. (c) The motor function of uninjured rats was unaffected by treatment with HAMC, □; or composite HAMC, ◆; up to 14 days, with all animals scoring 21/21 on the BBB scale ($n = 4$).

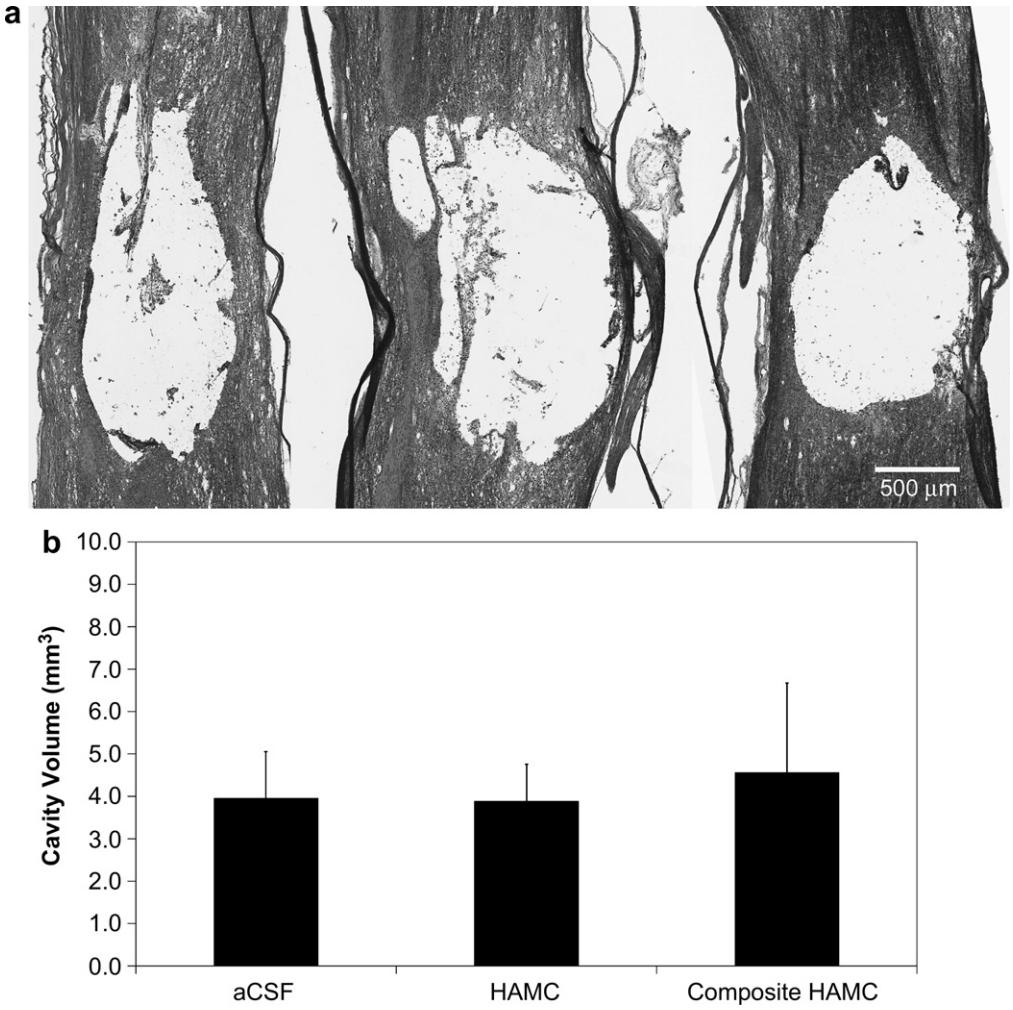

Fig. 3. a) Representative sections showing the injury cavity visualized with H&E and LFB staining at 28 days are shown for: aCSF, HAMC, and composite HAMC (left to right). b) There was no significant difference in the cavity volume between groups. Cavity volume was calculated from a series of weighted cavity area sections as-detailed in the Methods ($\geq$10 sections/animal, $n = 4$ animals, mean $\pm$ standard deviation shown).

were formulated with a reduced swelling ratio *in vitro* relative to previous formulations [26].

Unexpectedly, when HAMC had hydrophobic PLGA nanoparticles dispersed within it the modulus increased in a time-dependent manner suggestive of cross-link formation. In physically cross-linked composites this is often by hydrogen bonding, hydrophobic interaction, or ionic bonding [45]. A similar effect was observed when PLGA nanoparticles were dispersed in MC alone, suggesting that the nanoparticle-mediated stiffening is due to additional physical interactions between MC and PLGA. Importantly, composite MC is a reversible gel similar to MC alone (Fig. 1b) and composite HAMC remained injectable. This reversible inverse thermal gelation suggests that the specific MC-PLGA interaction is similar to the entropy driven self-association of MC, where previously ordered water molecules at the water-MC interface are freed, allowing MC–MC hydrophobic junctions to form, resulting in gelation [31]. Phenomenological reports of increased hydrogel stability of composite HAMC [26] suggest this interaction results in stable adsorption of MC to the PLGA particle surface.

PLGA nanoparticles were included in HAMC as a means to increase the duration of drug release beyond what is possible from the diffusion-controlled mechanism of a dissolved drug from HAMC alone [26], but their impact on the tissue response to HAMC was unknown. The current *in vivo* work allowed us to determine that PLGA nanoparticles in the composite were tolerated at the site of injection and that the enhanced stability of composite HAMC did not negatively affect the tissue response relative to previous reports of HAMC alone [19,23]. Our results contrast a previous study where suspensions of 5 µm PLGA microparticles, infused in the intrathecal space in a rat model, embedded in the pia mater and were found to trigger microglial activation in the meninx [41]. In the current study, one dose of composite HAMC contained twice the mass of PLGA and significantly smaller diameter particles (252 nm), relative to this previous report, yet, we did not observe a similar level of microglial activation.

The impact of composite HAMC vs. HAMC on the locomotor function (i.e. BBB score) of uninjured and injured rats were followed. When HAMC and composite HAMC were injected intrathecally in uninjured rats there was no effect on the BBB score, with each animal scoring 21/21 for the duration of the 14 day study. Given the perfect motor scores at 14 d, it is clear that any *in vivo* swelling of HAMC and composite HAMC did not affect motor function. After clip compression injury, there is some spontaneous recovery of motor function, and to be considered safe, an injected material must not reduce the degree of recovery. Spontaneous recovery is usually complete when the BBB score plateaus, typically

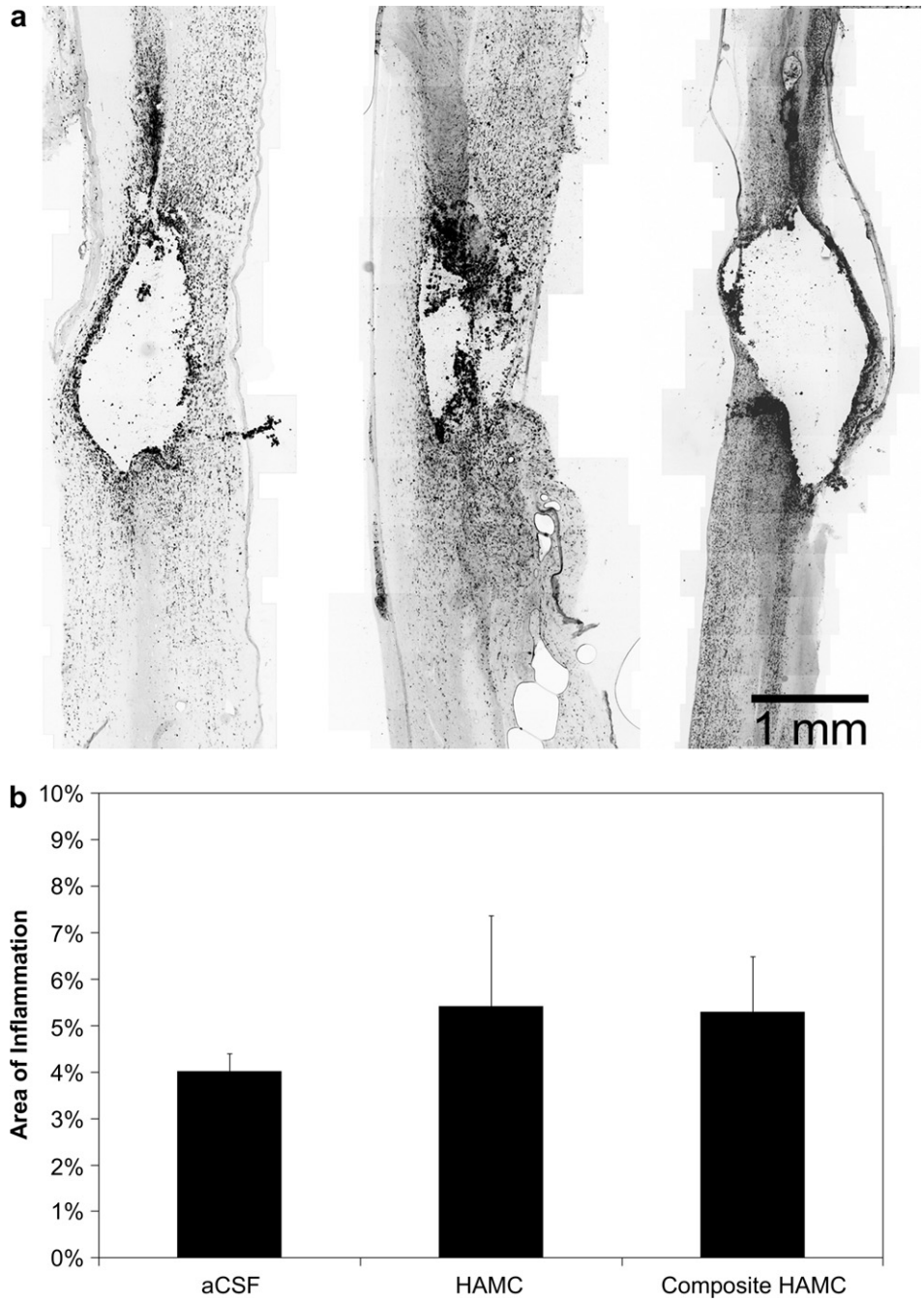

Fig. 4. a) Representative spinal cord sections showing ED-1 positive macrophages and microglia indicative of the inflammatory response 28 days after injection of: aCSF, HAMC, and composite HAMC (left to right). Pixel intensity has been inverted for clarity to show ED-1 staining (black) and surrounding tissue (grey). b) Area of inflammation was calculated as the fraction of ED-1 positive tissue in 20 mm parasagittal sections (200 mm^2 tissue/animal, $n = 4$ animals, mean $\pm$ standard deviation shown). There was no significant difference in the inflammatory response between groups.

between 21 and 28 days after injury [46]. When HAMC and composite HAMC were tested in SCI rats neither material significantly affected the BBB score (relative to aCSF injection) up to 28 days. These results are consistent with reports of lower molecular weight HAMC and collagen gels injected into the intrathecal space and suggest that the *in vivo* swelling behaviour of HAMC was safe in this application [19,20,22].

An acceptable local tissue response is an important factor in assessing the overall safety and biocompatibility of a biomaterial in a given application. We investigated inflammation within the spinal cord at the site of contact with the hydrogels because inflammation can result in neuronal death, astrogliosis, tissue adhesions, and impaired function [6,38]. Composite HAMC was of particular interest because PLGA can elicit a transient inflammatory response [50]. Uninjured animals that received HAMC showed negligible microglial activation at 14 days, but composite HAMC-treated animals showed mild to moderate ED-1 staining which may be a response to the PLGA particles within the hydrogel (Fig. 2). The magnitude of macrophage activation appears significantly less than that reported for PLGA microparticles implanted in intraperitoneal [39] and other soft tissue environments [38], consistent with the role of blood contact in the inflammatory response. We anticipated

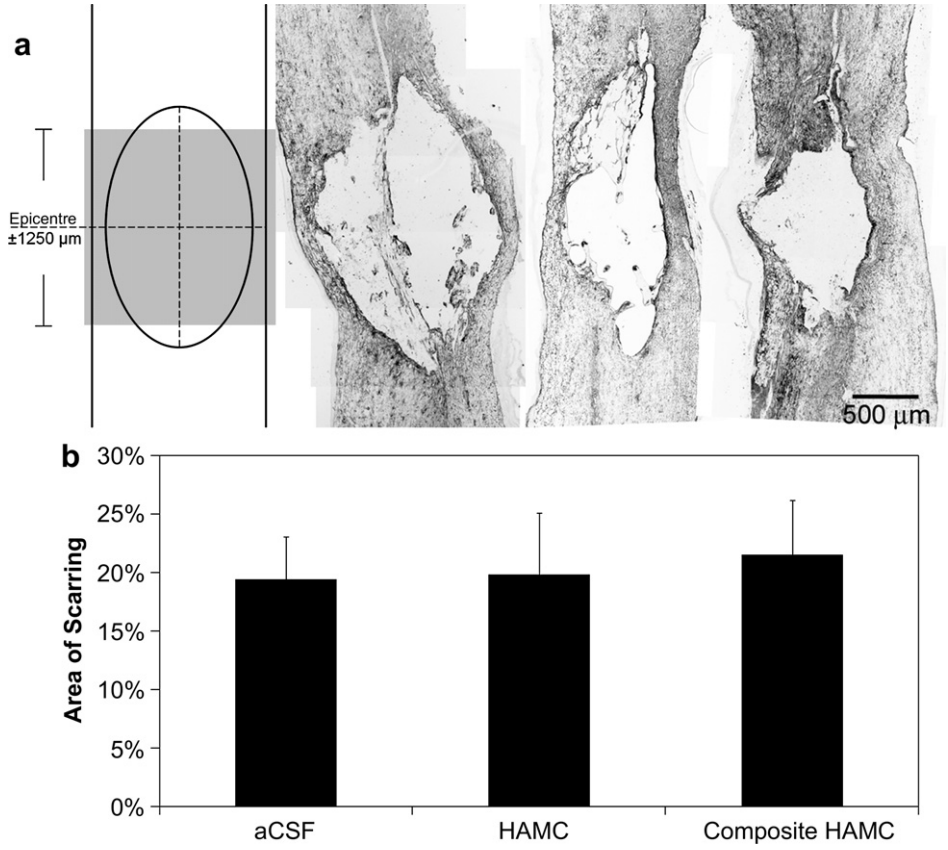

Fig. 5. a) Method for calculating area of glial scar and representative sections showing the glial scar *via* GFAP staining of astrocytes at 28 days are shown for: aCSF, HAMC, and composite HAMC (left to right). Method cartoon is not to scale. Pixel intensity has been inverted for clarity in print to show GFAP staining (black) and surrounding tissue (grey). b) Area of scarring was calculated as the fraction of GFAP positive tissue in a region encompassing the epicentre ±1.250 mm in parasagittal sections (10 mm^2 tissue/animal, $n = 4$ animals, mean ± standard deviation shown). There was no significant difference in the glial scar between groups.

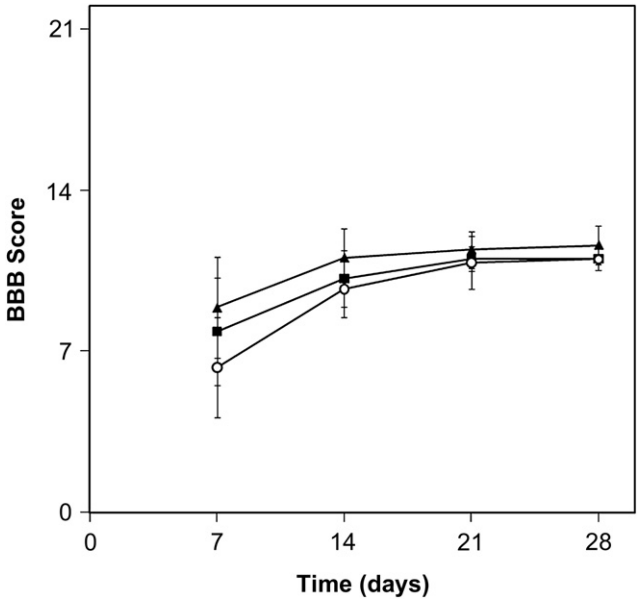

Fig. 6. Neither injection of HAMC nor composite HAMC significantly affected motor recovery relative to injection of aCSF after clip compression injury, suggesting the safety of these materials in their intended use as a drug delivery platform ($p > 0.01$ by ANOVA per time, $n = 10$). Composite HAMC, ○; HAMC, ■; and aCSF control, ▲.

any tissue response to PLGA in the composite HAMC subgroup would be mitigated relative to direct implantation because only a small fraction of the nanoparticles would be in contact with tissue, the majority being retained within the hydrogel. The slightly increased inflammatory response to composite HAMC vs. HAMC is likely due to the presence of PLGA nanoparticles; however, the increased modulus of composite HAMC relative to HAMC gel alone may also account for this increased tissue response. Substrate stiffness and the application of pressure to a tissue are known to alter cellular function [51].

Prominent ED-1 staining was found in all injured animals at 28 days, surrounding the cavity and rostro-caudally along the midline of the cord in a manner consistent with the injury response in the CNS [6,8]. No difference in microglial activation was found between HAMC and the aCSF control, with 4–5% of the tissue in injured animals positive for ED-1 in Fig. 4b. This lack of a significantly increased inflammatory response is in agreement with the known tissue response to HA, MC, and hydrogels in general [52]. The HAMC gel therefore has advantages over the biomaterials in current use by being fast gelling [26], non-adhesive [19], and minimally inflammatory in the intrathecal space after SCI. By comparison, collagen is well tolerated but cell-adhesive [53]; and cellulosic materials [35,54] or hyaluronan alone [55] are non-adhesive but not fast gelling. Importantly, there was no difference in microglial activation found between composite HAMC and the aCSF control or HAMC alone, consistent with reports of PLGA containing devices used in animal models of CNS injury [27–29]. It was not possible to determine if the qualitative increase in ED-1

staining observed in the pia mater of composite HAMC-treated uninjured rats at 14 days was also present in SCI rats at 28 days because the intrinsic inflammatory response to clip compression SCI dominated the tissue response.

Astrogliosis is the process of glial scar formation after SCI when astrocytes become activated, migrate to the site of injury and form a tight network bordering the cystic cavity. Proteoglycans, semaphorins, and other molecules within the glial scar biochemically inhibit neuroregeneration and plasticity [56,57]. Thus, we investigated astrocyte reactivity as a second element of the tissue response and biocompatibility because an increase in astrogliosis could confound regenerative therapies. Astrocyte activation was investigated using GFAP around the remaining rim of tissue nearest the injury epicentre, including both the internal surface of the cavity and exterior of the cord. The sections in Fig. 5a show that neither HAMC nor composite HAMC enhanced astrogliosis at the injection site on the dorsal cord. Quantitative analysis revealed no difference in the area of astrogliosis between groups, indicating that neither HAMC nor composite HAMC altered the area of tissue occupied by reactive astrocytes at 28 days. This result supports the use of HAMC materials in the intrathecal space.

Lastly, cavity volume after SCI is a gross measure of injury severity resulting from both the primary insult and secondary injury. If HAMC or composite HAMC induced a deleterious tissue response, such as apoptosis or an enhanced secondary injury cascade, cavity volume would increase. The insignificant difference in cavity volume between HAMC, composite HAMC and the aCSF control in Fig. 3b is in agreement with the locomotor testing reported in Fig. 6 and supports the conclusion that neither the composite HAMC nor HAMC alone affected the secondary injury processes associated with the extent of cavity formation relative to aCSF controls. This result, coupled with the insignificant differences in inflammation, astrogliosis and motor function in HAMC and composite HAMC-treated animals suggests that these materials are safe in the intrathecal space after SCI. These results are a significant milestone in the development of a sustained released drug delivery platform for treatment of SCI because composite HAMC allows local and sustained release of multiple therapeutics, with variable release rates, with one injection [26]. This strategy overcomes some of the limitations of other delivery techniques, such as bolus injection which is limited to short durations and pump/catheter which is limited by the potential for infection and scarring [58,59]. Having collected initial evidence that composite HAMC is safe and quantifying three aspects of biocompatibility, delivery studies using drug-loaded PLGA nanoparticles in HAMC are currently being pursued.

5. Conclusions

The inclusion of PLGA nanoparticles into physical hydrogels of HA and MC significantly altered the rheological properties of the HAMC gel, most likely through additional hydrophobic interactions between MC methyl groups and PLGA nanoparticles. This interaction explains the increase in stability of composite HAMC relative to HAMC alone. The hydrogel and particle loaded composite are well tolerated in the intrathecal space of uninjured rats for 14 days post-injection with minimal microglial activation and no effect on locomotor BBB score. The local tissue response in rats with clip compression SCI showed no significant increase in microglial activation, astrocytic response, or cystic cavity volume due to HAMC or composite HAMC relative to aCSF at 28 days after injury. The safety of these materials in the intrathecal space was supported by similar motor function in rats with SCI that received aCSF, HAMC or composite HAMC as-measured by the BBB scale. This work provides initial evidence supporting the safety and biocompatibility of composite HAMC as a platform for sustained combination therapy to the injured spinal cord.

Acknowledgements

We are grateful to CIHR MOP# 44054 for funding (MSS, CHT). MDB acknowledges NSERC for a CGSD scholarship. The authors are indebted to Peter Poon for his surgical and immunohistochemical expertise; and to Siang Liao Lee, Ankeeta Tadkase, and Valerie Peng for their skilled tissue processing and microscopy.

References

[1] Tator CH. Experimental and clinical studies of the pathophysiology and management of acute spinal cord injury. J Spinal Cord Med 1996;19(4):206–14.
[2] Girard C, Bemelmans AP, Dufour N, Mallet J, Bachelin C, Nait-Oumesmar B, et al. Grafts of brain-derived neurotrophic factor and neurotrophin 3-transduced primate Schwann cells lead to functional recovery of the demyelinated mouse spinal cord. J Neurosci 2005;25(35):7924–33.
[3] Rabchevsky AG, Fugaccia I, Fletcher-Turner A, Blades DA, Mattson MP, Scheff SW. Basic fibroblast growth factor (bFGF) enhances tissue sparing and functional recovery following moderate spinal cord injury. J Neurotrauma 1999;16(9):817–30.
[4] Schwab ME. Nogo and axon regeneration. Curr Opin Neurobiol 2004;14(1):118–24.
[5] Fitch MT, Doller C, Combs CK, Landreth GE, Silver J. Cellular and molecular mechanisms of glial scarring and progressive cavitation: in vivo and in vitro analysis of inflammation-induced secondary injury after CNS trauma. J Neurosci 1999;19(19):8182–98.
[6] Stroncek JD, Reichert WM. Overview of wound healing in different tissue types. In: Reichert W, editor. Indwelling neural implants: strategies for contending with the in vivo environment. Boca Raton: CRC Press; 2008.
[7] Ramer LM, Ramer MS, Steeves JD. Setting the stage for functional repair of spinal cord injuries: a cast of thousands. Spinal Cord 2005;43(3):134–61.
[8] Donnelly DJ, Popovich PG. Inflammation and its role in neuroprotection, axonal regeneration and functional recovery after spinal cord injury. Exp Neurol 2008;209(2):378–88.
[9] Bradbury EJ, Khemani S, Von R, King, Priestley JV, McMahon SB. NT-3 promotes growth of lesioned adult rat sensory axons ascending in the dorsal columns of the spinal cord. Eur J Neurosci 1999;11(11):3873–83.
[10] Tuszynski MH, Grill R, Jones LL, Brant A, Blesch A, Low K, et al. NT-3 gene delivery elicits growth of chronically injured corticospinal axons and modestly improves functional deficits after chronic scar resection. Exp Neurol 2003;181(1):47–56.
[11] Tobias CA, Shumsky JS, Shibata M, Tuszynski MH, Fischer I, Tessler A, et al. Delayed grafting of BDNF and NT-3 producing fibroblasts into the injured spinal cord stimulates sprouting, partially rescues axotomized red nucleus neurons from loss and atrophy, and provides limited regeneration. Exp Neurol 2003;184(1):97–113.
[12] Zahir T, Chen YF, MacDonald JF, Leipzig N, Tator CH, Shoichet MS. Neural stem/progenitor cells differentiate in vitro to neurons by the combined action of dibutyryl cAMP and interferon-gamma. Stem Cells Dev 2009;18(10):1423–32.
[13] Hawryluk G, Karmimi-Abdolrezaee S, Eftekharpour E, Fehlings M. Examination of the early effects of neural precursor cell transplantation on the perilesional environment of the injured spinal cord. J Neurotrauma 2008;25(7):P296.
[14] Chvatal SA, Kim YT, Bratt-Leal AM, Lee H, Bellamkonda RV. Spatial distribution and acute anti-inflammatory effects of Methylprednisolone after sustained local delivery to the contused spinal cord. Biomaterials 2008;29(12):1967–75.
[15] Jain A, Kim YT, McKeon RJ, Bellamkonda RV. In situ gelling hydrogels for conformal repair of spinal cord defects, and local delivery of BDNF after spinal cord injury. Biomaterials 2006;27(3):497–504.
[16] Wang YC, Wu YT, Huang HY, Lin HI, Lo LW, Tzeng SF, et al. Sustained intraspinal delivery of neurotrophic factor encapsulated in biodegradable nanoparticles following contusive spinal cord injury. Biomaterials 2008;29(34):4546–53.
[17] Tator CH. Review of treatment trials in human spinal cord injury: issues, difficulties, and recommendations. Neurosurgery 2006;59(5):957–82. discussion: 982–7.
[18] Straley KS, Foo CW, Heilshorn SC. Biomaterial design strategies for the treatment of spinal cord injuries. J Neurotrauma 2010;27(1):1–19.
[19] Gupta D, Tator CH, Shoichet MS. Fast-gelling injectable blend of hyaluronan and methylcellulose for intrathecal, localized delivery to the injured spinal cord. Biomaterials 2006;27(11):2370–9.
[20] Jimenez Hamann MC, Tsai EC, Tator CH, Shoichet MS. Novel intrathecal delivery system for treatment of spinal cord injury. Exp Neurol 2003;182(2):300–9.
[21] Ballios BG, Cooke MJ, van der Kooy D, Shoichet MS. A hydrogel-based stem cell delivery system to treat retinal degenerative diseases. Biomaterials 2010;31(9):2555–64.

[22] Jimenez Hamann MC, Tator CH, Shoichet MS. Injectable intrathecal delivery system for localized administration of EGF and FGF-2 to the injured rat spinal cord. Exp Neurol 2005;194(1):106–19.
[23] Kang CE, Poon PC, Tator CH, Shoichet MS. A new paradigm for local and sustained release of therapeutic molecules to the injured spinal cord for neuroprotection and tissue repair. Tissue Eng Part A 2009;15(3):595–604.
[24] Norenberg MD, Smith J, Marcillo A. The pathology of human spinal cord injury: Defining the problems. J Neurotrauma 2004;21(4):429–40.
[25] Fehlings MG, Perrin RG. The timing of surgical intervention in the treatment of spinal cord injury: a systematic review of recent clinical evidence. Spine 2006;31(11 Suppl.):S28–35. discussion: S36.
[26] Baumann MD, Kang CE, Stanwick JC, Wang Y, Kim H, Lapitsky Y, et al. An injectable drug delivery platform for sustained combination therapy. J Control Release 2009;138(3):205–13.
[27] Wong DY, Hollister SJ, Krebsbach PH, Nosrat C. Poly(epsilon-caprolactone) and poly (L-lactic-co-glycolic acid) degradable polymer sponges attenuate astrocyte response and lesion growth in acute traumatic brain injury. Tissue Eng 2007;13(10):2515–23.
[28] Fournier E, Passirani C, Montero-Menei CN, Benoit JP. Biocompatibility of implantable synthetic polymeric drug carriers: focus on brain biocompatibility. Biomaterials 2003;24(19):3311–31.
[29] Kou JH, Emmett C, Shen P, Aswani S, Iwamoto T, Vaghefi F, et al. Bioerosion and biocompatibility of poly(d, l-lactic-co-glycolic acid) implants in brain. J Control Release 1997;43(2–3):123–30.
[30] Lemons ML, Howland DR, Anderson DK. Chondroitin sulfate proteoglycan immunoreactivity increases following spinal cord injury and transplantation. Exp Neurol 1999;160(1):51–65.
[31] Sarkar N. Kinetics of thermal gelation of methylcellulose and hydroxypropylmethylcellulose in aqueous-solutions. Carbohydr Polym 1995;26 (3):195–203.
[32] Zheng PJ, Li L, Hu X, Zhao XY. Sol–gel transition of methylcellulose in phosphate buffer saline solutions. J Poly Sci B Polym Phys 2004;42(10):1849–60.
[33] Tate MC, Shear DA, Hoffman SW, Stein DG, LaPlaca MC. Biocompatibility of methylcellulose-based constructs designed for intracerebral gelation following experimental traumatic brain injury. Biomaterials 2001;22(10): 1113–23.
[34] Kang CE, Tator CH, Shoichet MS. Poly(ethylene glycol) modification enhances penetration of fibroblast growth factor 2 to injured spinal cord tissue from an intrathecal delivery system. J Control Release 2010;144(1):25–31.
[35] Topsakal C, Akpolat N, Erol FS, Ozveren MF, Akdemir I, Kaplan M, et al. Seprafilm superior to Gore-Tex in the prevention of peridural fibrosis. J Neurosurg 2004;101(2):295–302.
[36] Kato T, Haro H, Komori H, Shinomiya K. Evaluation of hyaluronic acid sheet for the prevention of postlaminectomy adhesions. Spine J 2005;5(5):479–88.
[37] Jiang D, Liang J, Noble PW. Hyaluronan in tissue injury and repair. Annu Rev Cell Dev Biol 2007;23:435–61.
[38] Anderson JM, Shive MS. Biodegradation and biocompatibility of PLA and PLGA microspheres. Adv Drug Deliv Rev 1997;28(1):5–24.
[39] Kohane DS, Tse JY, Yeo Y, Padera R, Shubina M, Langer R. Biodegradable polymeric microspheres and nanospheres for drug delivery in the peritoneum. J Biomed Mater Res A 2006;77(2):351–61.
[40] Domnina YA, Yeo Y, Tse JY, Bellas E, Kohane DS. Spray-dried lipid–hyaluronan–polymethacrylate microparticles for drug delivery in the peritoneum. J Biomed Mater Res A 2008;87(3):825–31.
[41] Soderquist RG, Sloane EM, Loram LC, Harrison JA, Dengler EC, Johnson SM, et al. Release of plasmid DNA-encoding IL-10 from PLGA microparticles facilitates long-term reversal of neuropathic pain following a single intrathecal administration. Pharm Res 2010;27 (5):841–54.
[42] Rivlin AS, Tator CH. Effect of duration of acute spinal cord compression in a new acute cord injury model in the rat. Surg Neurol 1978;10(1):38–43.
[43] Basso DM, Beattie MS, Bresnahan JC. A sensitive and reliable locomotor rating scale for open field testing in rats. J Neurotrauma 1995;12(1):1–21.
[44] Schupper N, Rabin Y, Rosenbluh M. Multiple stages in the aging of a physical polymer gel. Macromolecules 2008;41(11):3983–94.
[45] Schexnailder P, Schmidt G. Nanocomposite polymer hydrogels. Colloid Polym Sci 2009;287(1):1–11.
[46] Poon PC, Gupta D, Shoichet MS, Tator CH. Clip compression model is useful for thoracic spinal cord injuries: histologic and functional correlates. Spine 2007;32(25):2853–9.
[47] Kobayashi Y, Okamoto A, Nishinari K. Viscoelasticity of hyaluronic acid with different molecular weights. Biorheology 1994;31(3):235–44.
[48] Fehlings MG. The impact of continued cord compression following traumatic spinal cord injury. J Neurosurg Spine 2009;11(5):568–9.
[49] Nowak DD, Lee JK, Gelb DE, Poelstra KA, Ludwig SC. Central cord syndrome. J Am Acad Orthop Surg 2009;17(12):756–65.
[50] Athanasiou KA, Niederauer GG, Agrawal CM. Sterilization, toxicity, biocompatibility and clinical applications of polylactic acid polyglycolic acid copolymers. Biomaterials 1996;17(2):93–102.
[51] Janmey PA, Winer JP, Murray ME, Wen Q. The hard life of soft cells. Cell Motil Cytoskeleton 2009;66(8):597–605.
[52] Wheeler JC, Woods JA, Cox MJ, Cantrell RW, Watkins FH, Edlich RF. Evolution of hydrogel polymers as contact lenses, surface coatings, dressings, and drug delivery systems. J Long Term Eff Med Implants 1996;6(3–4):207–17.
[53] Preul MC, Bichard WD, Muench TR, Spetzler RF. Toward optimal tissue sealants for neurosurgery: use of a novel hydrogel sealant in a canine durotomy repair model. Neurosurgery 2003;53(5):1189–98.
[54] Haq I, Cruz-Almeida Y, Siqueira EB, Norenberg M, Green BA, Levi AD. Postoperative fibrosis after surgical treatment of the porcine spinal cord: a comparison of dural substitutes. J Neurosurg Spine 2005;2(1):50–4.
[55] Yeo Y, Ito T, Bellas E, Highley CB, Marini R, Kohane DS. In situ cross-linkable hyaluronan hydrogels containing polymeric nanoparticles for preventing postsurgical adhesions. Ann Surg 2007;245(5):819–24.
[56] Fawcett JW. Overcoming inhibition in the damaged spinal cord. J Neurotrauma 2006;23(3–4):371–83.
[57] Rhodes KE, Fawcett JW. Chondroitin sulphate proteoglycans: preventing plasticity or protecting the CNS? J Anat 2004;204(1):33–48.
[58] Jones LL, Tuszynski MH. Chronic intrathecal infusions after spinal cord injury cause scarring and compression. Microsc Res Tech 2001;54(5):317–24.
[59] McCall TD, MacDonald JD. Cervical catheter tip placement for intrathecal baclofen administration. Neurosurgery 2006;59(3):634–40. discussion: 634–40.